

CHAPTER III

RESULTS AND DISCUSSION

3.1 Alpha Transition Temperature

The measurement of transition temperature can assist in the determination of compatibility of amorphous polymer blends (Folkes and Hope, 1993). Immiscible blends usually show two T_g 's characteristic, one for each phase. The addition of diblock copolymer will reduce the number of unfavorable contacts and mediates enthalpic interaction between the two polymers, and enhance the degree of compatibility of the polymer blend. If a blend becomes more compatible, the transition temperature of each phase would shift closer together.

Figure 3.1 shows loss modulus of PS/PI (40/60) blends as a function of temperature and the diblock copolymer content. The maxima in loss modulus (G'') was used as the definition of the alpha transition temperature (T_α). For the α -transition the portion of molecule excited may be from 10 to 50 atoms or more (Brandruys and Immergut, 1975). Alpha transition temperature (T_α) is associated with the glass transition temperature (T_g). T_g indicates the change in the heat capacity which reflects a fundamental change in molecule motion (Spherling, 1993). We observed two peaks, one for each phase; they are called the rubber phase peak ($T_\alpha \approx -57^\circ\text{C}$) and the hard phase peak ($T_\alpha \approx 90^\circ\text{C}$). Our PS/P(S-b-I)/PI blends system is composed of a rubber phase and a hard phase; the rubber phase is PI homopolymers and PI segments, the hard phase is PS homopolymers and PS segments.

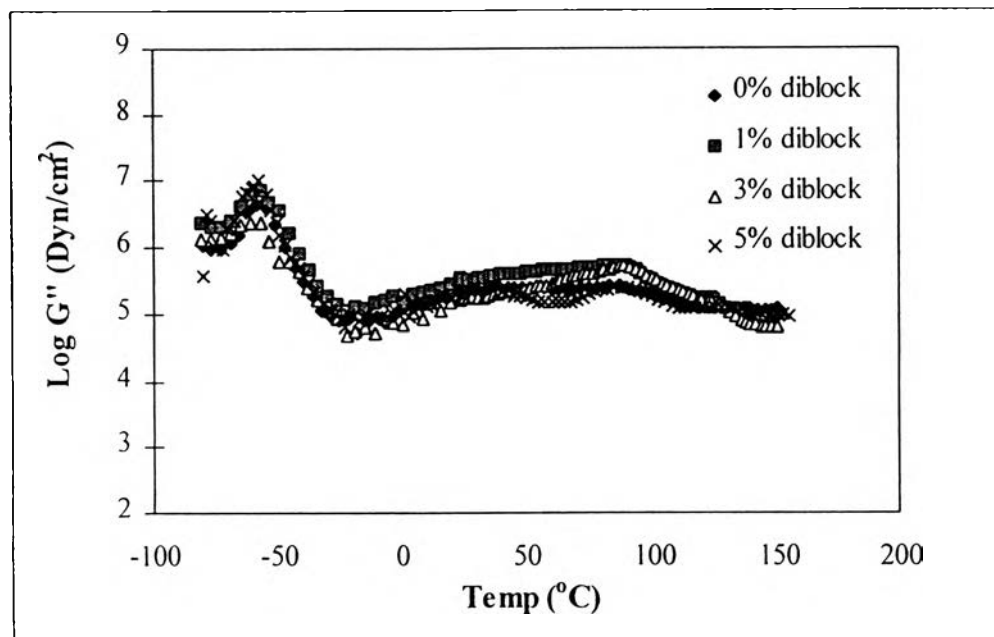


Figure 3.1 Loss modulus of PS/PI (40/60) blends as a function of temperature and the diblock copolymer content.

3.1.1 Effect of the diblock copolymer content on the alpha transition temperature of PS/PI blends

To study the effect of the diblock copolymer concentration on the alpha transition temperature, the composition for the PS/PI blends was fixed at 40/60 and the diblock copolymer concentration was varied from 0-5 wt %.

Figure 3.2 shows the effect of the diblock copolymer content on the alpha transition temperature of the rubber phase of the blends. The alpha transition temperatures of the rubber phase are nearly the same with additions of diblock copolymer between 1-5 wt %.

Figure 3.3 shows the effect of the diblock copolymer content on the alpha transition temperature of the hard phase of the blends. There is no change in the alpha transition temperature with additions of the diblock copolymer between 1-5 wt %.

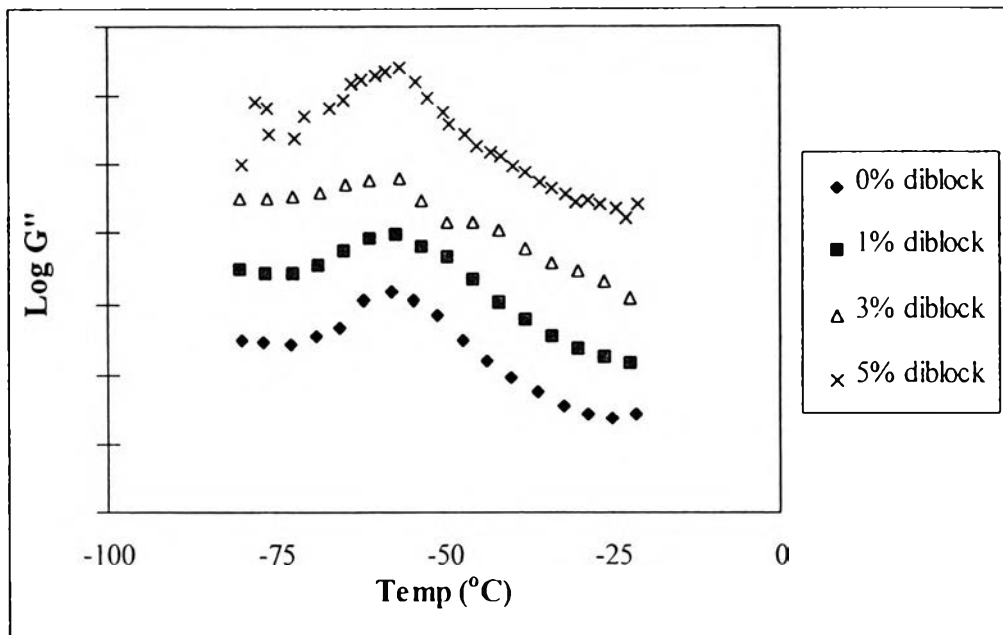


Figure 3.2 Effect of the diblock copolymer content on the alpha transition temperature of the rubber phase of PS/PI (40/60) blends.

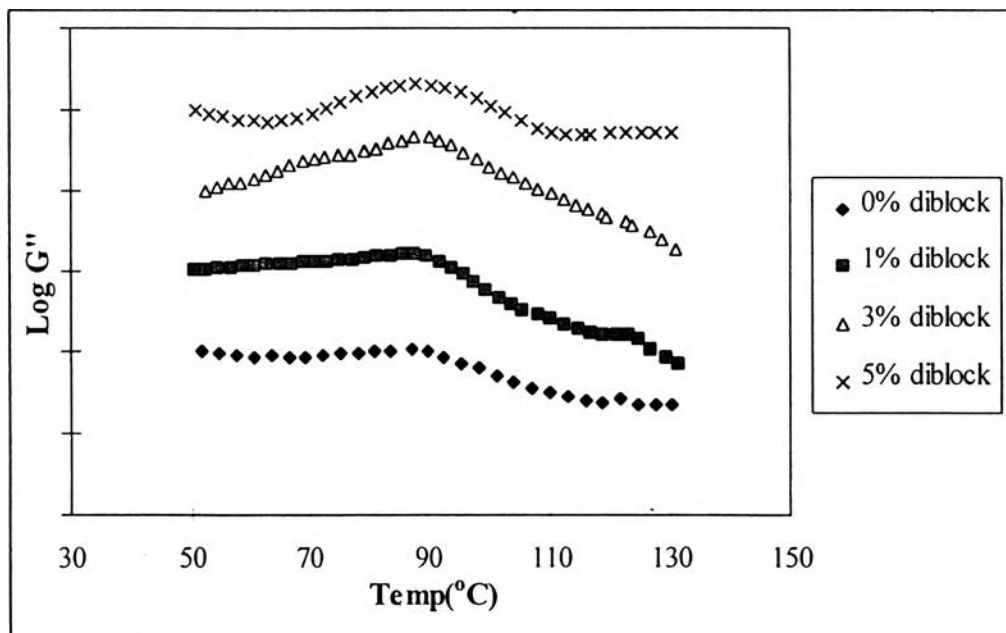


Figure 3.3 Effect of the diblock copolymer content on the alpha transition temperature of the hard phase of PS/PI (40/60) blends.

Table 3.1 Effect of the diblock copolymer on the alpha transition temperature of PS/PI (40/60) blends

| Diblock copolymer | T_{α} of rubber phase | T_{α} of hard phase | ΔT_{α} |
|-------------------|------------------------------|----------------------------|---------------------|
| 0% | -57.1 | 89.8 | 146.9 |
| 1% | -56.9 | 89.7 | 146.6 |
| 3% | -56.7 | 90.0 | 146.7 |
| 5% | -56.5 | 89.1 | 145.6 |

Table 3.1 depicts the alpha transition temperature for each phase and the difference between the two alpha transition temperatures (ΔT_{α}). ΔT_{α} is not significantly changed with additions of any diblock copolymer contents.

We did not see a change in the alpha transition temperature because our blend is nearly symmetric in composition. Any small amounts of diblock copolymer content added would only influence a small interfacial volume between the two phases. Therefore a relatively large portion of each phase was unaltered, and T_{α} 's remained unchanged. The second reason is that T_g of PS homopolymer and PS segment is the same. It is difficult to observe change in the alpha transition temperature. It should be noted that the undetectable change in the alpha transition temperature does not mean that the blends were not compatibilized or interfacial adhesion was not enhanced.

3.1.2 Effect of the diblock copolymer content on the alpha transition temperature of PPO/PI blends

The effect of the diblock copolymer content on the alpha transition temperature of PPO/PI blends was studied for the composition ratio of 40/60 and the diblock copolymer concentration was varied from 0-5 wt %. PPO/P(S-

b-I)/PI blends are composed of a rubber phase and a hard phase, where the rubber phase is PI homopolymers and PI segments, the hard phase is PPO homopolymers and PS segments.

Figure 3.4 shows the effect of the diblock copolymer content on the alpha transition temperature of the rubber phase of the blends. The alpha transition temperature of the rubber phase shifts toward a higher temperature as diblock copolymer concentration increases.

Figure 3.5 shows the effect of diblock the copolymer content on the alpha transition temperature of the hard phase of the blends. The alpha transition temperature of the hard phase shifts toward a lower temperature as more diblock copolymer is added.

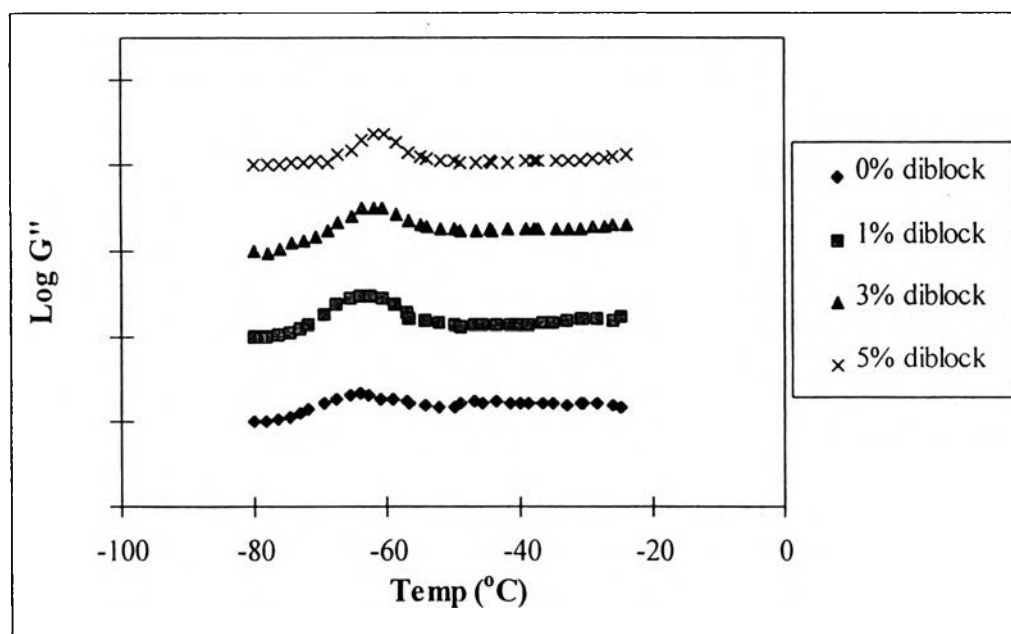


Figure 3.4 Effect of the diblock copolymer content on the alpha transition temperature of rubber phase of PPO/PI (40/60) blends.

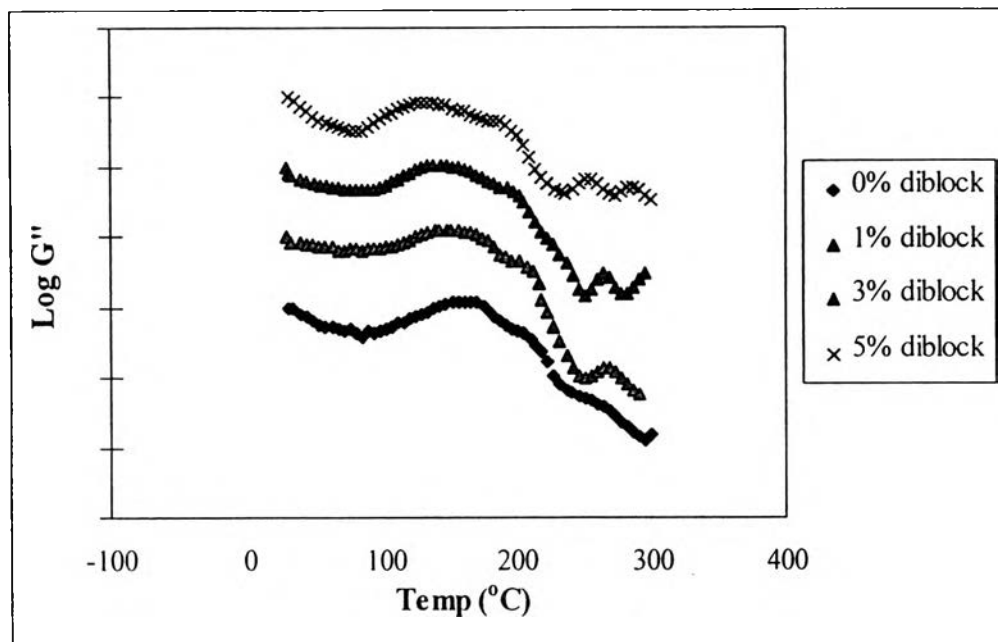


Figure 3.5 Effect of the diblock copolymer content on the alpha transition temperature of the hard phase of PPO/PI (40/60) blends.

Table 3.2 Effect of the diblock copolymer on the alpha transition temperature of PPO/PI (40/60) blends

| Diblock copolymer | T_{α} of rubber phase | T_{α} of hard phase | ΔT_{α} |
|-------------------|------------------------------|----------------------------|---------------------|
| 0% | -64.2 | 162.9 | 227.1 |
| 1% | -63.8 | 149.3 | 213.0 |
| 3% | -61.9 | 142.9 | 204.8 |
| 5% | -60.0 | 135.8 | 195.8 |

Table 3.2 shows the alpha transition temperature values of each phase and the difference between the two alpha transition temperatures (ΔT_{α}).

We can see that T_{α} of each phase shifts closer together as more diblock copolymer is added. In the previous work of Tucker and Barlow (1988), they found that PPO and PS are miscible at all compositions, hence T_{α} of the PPO homopolymer and the PS segment blends has a single T_{α} between T_{g} s of PPO and PS. From our experiment, T_{α} 's of the hard phase shifts are due to this reason. The basic miscibility of PS and PPO is an exothermic heat of mixing; this introduces a new driving force for mixing with styrene blocks of P(S-b-I) that does not exist in the previous case with PS homopolymer. Hence the influence of exothermic interaction between PPO homopolymer and PS segment induces the alpha transition temperature of the hard phase to shift to lower temperatures.

It is surprising to find that the effect of the exothermic heat of mixing can induce some change in the alpha transition temperature of the rubber phase as well. Apparently the strong expansion of the PS segments due to PPO interaction also result in some stiffening of the PI segments.

Finally, we note that the side groups of PS and PPO are benzene groups that are large side groups. The β peak shows torsional vibration of the benzene group. Thus the alpha transition temperature of the hard phase of the blends involves both β peak and α peak leading to a single broad peak.

3.2 Young's Modulus

Young's modulus was obtained from the initial slope of stress and strain curve. It can be used to infer an adhesion between phases. The Young's modulus was examined by using a highest force rate of 500 mN/min to minimize relaxation of the samples. The composition of PS/PI or PPO/PI blends was fixed at 40/60 and the diblock copolymer concentration was varied from 0-5 wt %.

3.2.1 Effect of the diblock copolymer content on the Young's modulus of PS/PI blends

a) PS/PI in the Glassy/Rubbery state

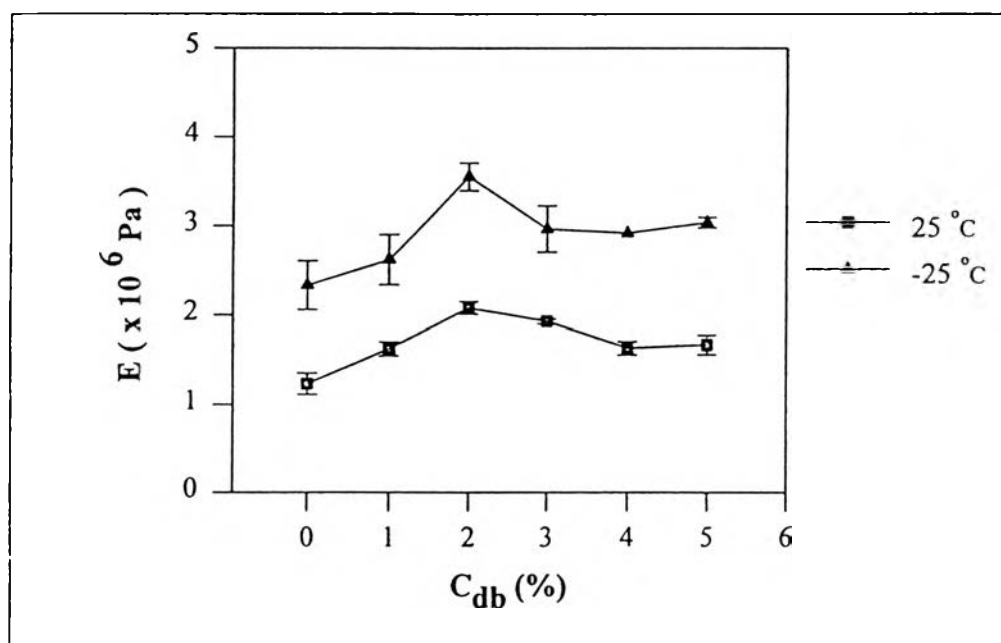


Figure 3.6 Effect of the diblock copolymer content on the Young's modulus of PS/PI (40/60) blends at 25 °C and -25 °C.

Figure 3.6 shows the effect of the diblock copolymer content on the Young's modulus of the blends at 25 °C and -25 °C. At these temperatures, the PS phase is in the glassy state and the PI phase is in the rubbery state. At the lower temperature, the Young's modulus is greater because the polymer chains are more restricted, and the resistance to stretching is greater. From figure 3.6, the Young's modulus increases with the diblock copolymer concentration until it reaches the maximum value at 2 wt % of the diblock copolymer, then decreases toward an asymptotic value.

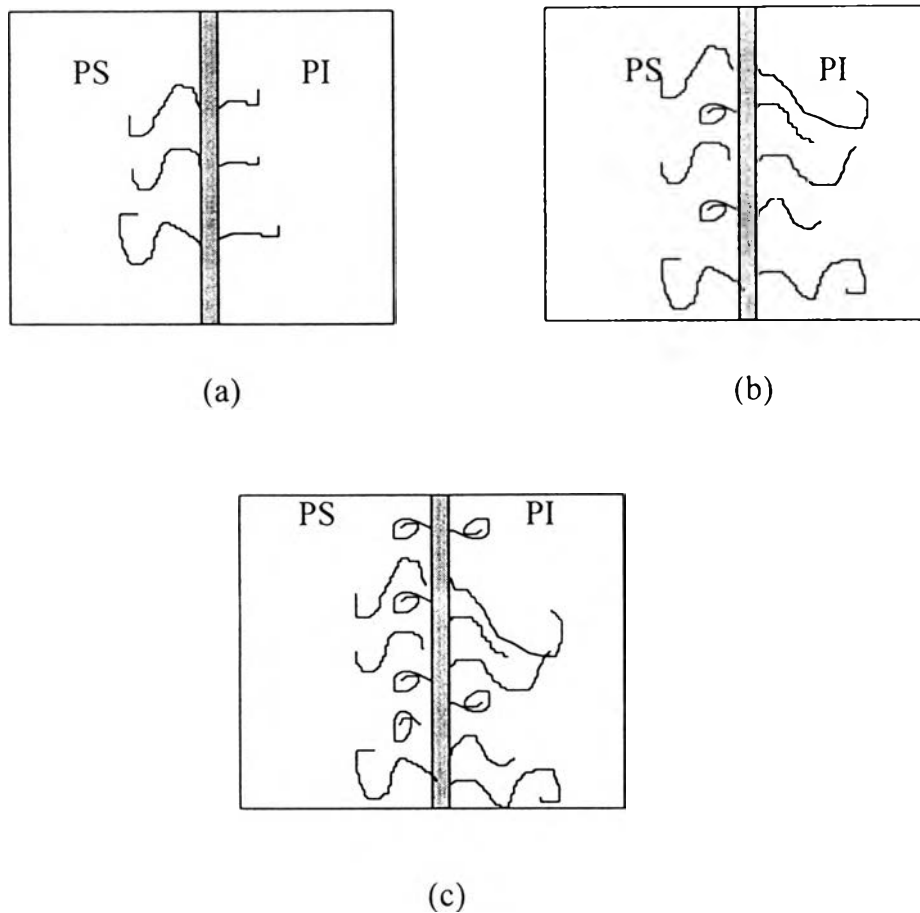


Figure 3.7 Ideal interfacial morphology model of PS/PI (40/60) blends as a function of the diblock copolymer content: a) 0-2 wt % , b) 2-3 wt % and c) 3-5 wt % of the diblock copolymer.

From Figures 3.6 and 3.7, between 0 wt % to 2 wt % of the diblock copolymer, the Young's modulus increases as diblock copolymer is added. The molecular weight ratio of homopolymer to block segment is 0.74 for PS/PS, and 13.7 for PI/PI. This means that the entropic swelling of the PS segments at the PS/PS interface is more favorable than that of the PI/PI interface. PS is rigid and has a higher Young's modulus, therefore the rigidity of PS can be more easily transferred to the blends producing the increase of the Young's modulus.

Beyond 2 wt % of the diblock copolymer concentration, it seems likely that the block copolymer tends to form micelles rather than add to the interface. The PI segments penetration became more dominant, and the rubbery property of PI can be transferred back to the blends producing a lowering of the Young's modulus.

Between 3 wt % to 5 wt % of the diblock copolymer, the Young's modulus is independent of the diblock copolymer content. This is probably because the block copolymer forms micelles rather than increase the interfacial area.

b) PS/PI in the Glassy/Glassy state

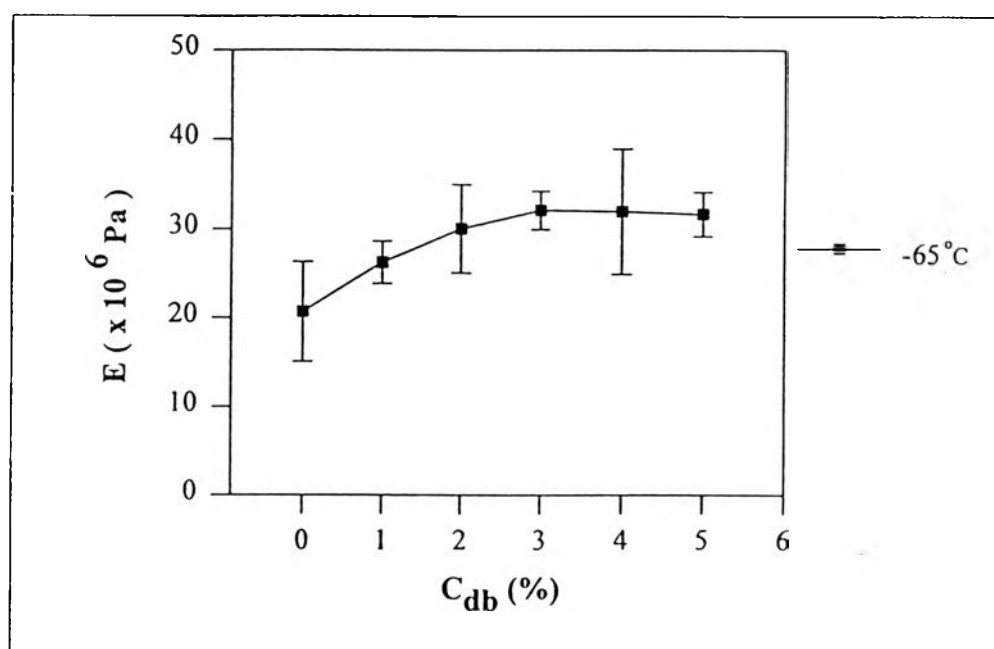


Figure 3.8 Effect of the diblock copolymer content on the Young's modulus of PS/PI (40/60) blends at -65 °C.

Figure 3.8 shows the effect of the diblock copolymer content on the Young's modulus of the blends at -65 °C. At this temperature, both of the PS and the PI phases are in the glassy state. The ideal interfacial morphology

model of glassy/glassy state is identical to that of glassy/rubbery state as shown in Figure 3.7.

This figure shows that the Young's modulus increases monotonously with wt % diblock copolymer up to 3 wt % of the diblock copolymer content. Beyond 3 wt % of the diblock copolymer content, the Young's modulus remains the same.

This result is different from that when PI in the rubbery state. The possible reason is due to the difference in the disentanglement between the PI homopolymers and PI segments while under extension. Disentanglement was more difficult at $-65\text{ }^{\circ}\text{C}$ than at $25\text{ }^{\circ}\text{C}$.

3.2.2 Effect of the diblock copolymer on the Young's modulus of PPO/PI (40/60) blends

a) PPO/PI in the Glassy/Rubbery state

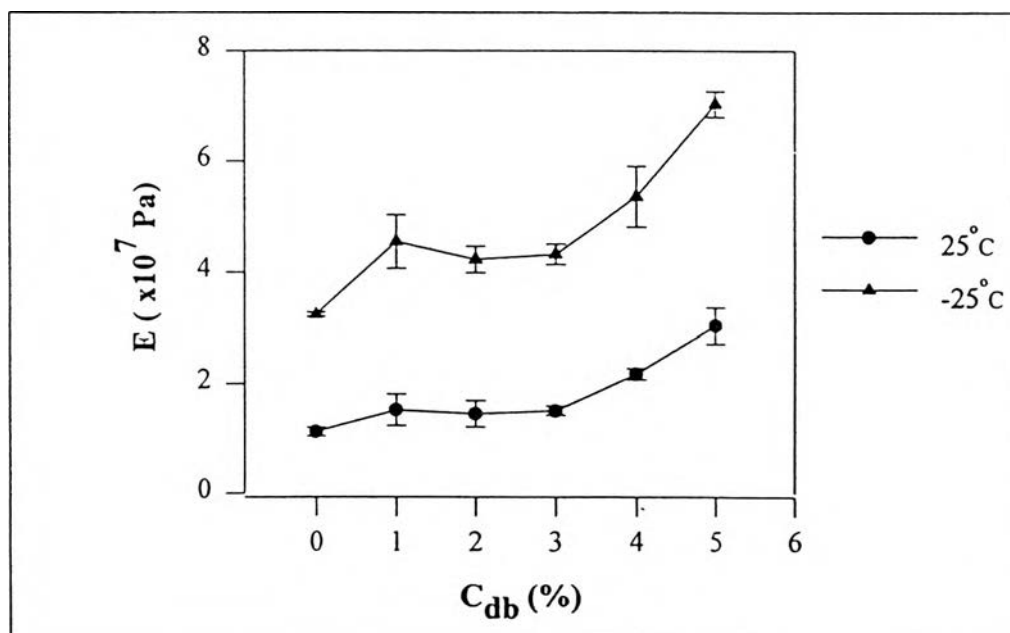


Figure 3.9 Effect of diblock copolymer content on Young's modulus of PPO/PI (40/60) blends at $25\text{ }^{\circ}\text{C}$ and $-25\text{ }^{\circ}\text{C}$.

Figure 3.9 shows the Young's modulus of PPO/PI (40/60) as a function of diblock content at 25 °C and -25 °C. At these temperatures, PPO is in the glassy state and PI is in the rubbery state. From Figure 3.9, the Young's modulus increases with the 1 wt % of the diblock copolymer concentration. Between 1 wt % to 3 wt % of the diblock copolymer, the Young's modulus does not change very much. Beyond 3 wt % of the diblock copolymer, the Young's modulus increases monotonously as diblock copolymer is added.

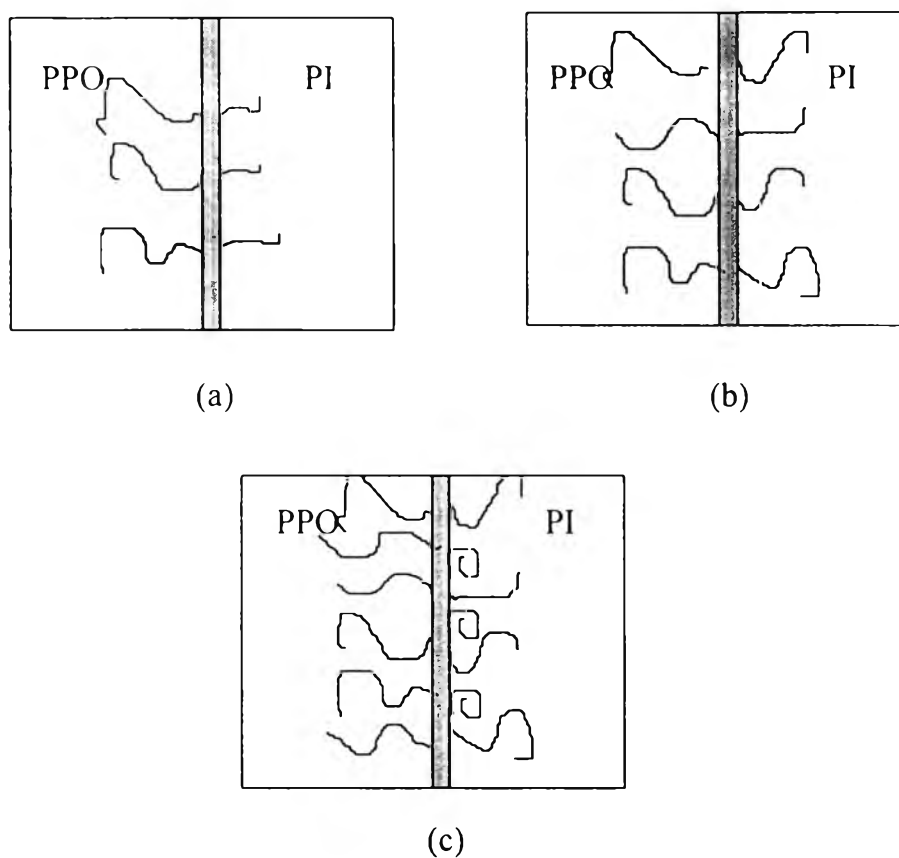


Figure 3.10 Ideal interfacial morphology model of PPO/PI (40/60) blends as a function of the diblock copolymer content: a) 0-1 wt % b) 1-3 wt % and c) 3-5 wt % of the diblock copolymer.

From Figures 3.9 and 3.10, at low diblock copolymer concentration, the Young's modulus increases as diblock copolymer is added. The reason is that the molecular weight ratio of the homopolymer to block copolymer is 0.74 for PPO/PS, and 13.7 for PI/PI, thus the extent of penetration of the PS segments into PPO is better than that of the PI segments. PPO is hard and has a higher Young's modulus, and the diblock copolymer acts as a phase linker between two phases inducing the increase of the Young's modulus.

Between 1 wt % to 3 wt % of the diblock copolymer, there is a balance in the penetration of the PS and PI segments into the homopolymer and the transfer of stress across the interface is dominated by both phases. Hence the Young's modulus seems to remain the same.

Between 3 wt % to 5 wt % of the diblock copolymer, the Young's modulus increases monotonously as diblock copolymer is added. That is not the same as the case of PS/P(S-b-I)PI blends in which the Young's modulus settles down toward the asymptotic value as shown in Figure 3.6. Because the interaction of the PS segment and PPO homopolymer is the exothermic heat of mixing, it introduces a driving force for mixing that does not exist in the case of the PS homopolymer. Therefore the PS segments penetrate more effectively into PPO homopolymers and do not so readily form micelles. There is a good interfacial adhesion between PS segments and PPO homopolymers. The hard property of PPO transfers to the blends, inducing the Young's modulus to increase.

b) PPO/PI in the Glassy/Glassy state

Figure 3.11 depicts the effect of the diblock copolymer content on the Young's modulus at -65°C . For this condition all polymers are in the glassy state. The ideal interfacial morphology model of glassy/glassy state is identical to that of glassy/rubbery state as shown in Figure 3.10.

From Figures 3.10 and 3.11, the Young's modulus increases with 1 % of the diblock copolymer. Between 1 wt % to 3 wt % of the diblock copolymer, the Young's modulus remains the same. Beyond 3 wt % of the diblock copolymer, the Young's modulus increases monotonously as more diblock copolymer is added.

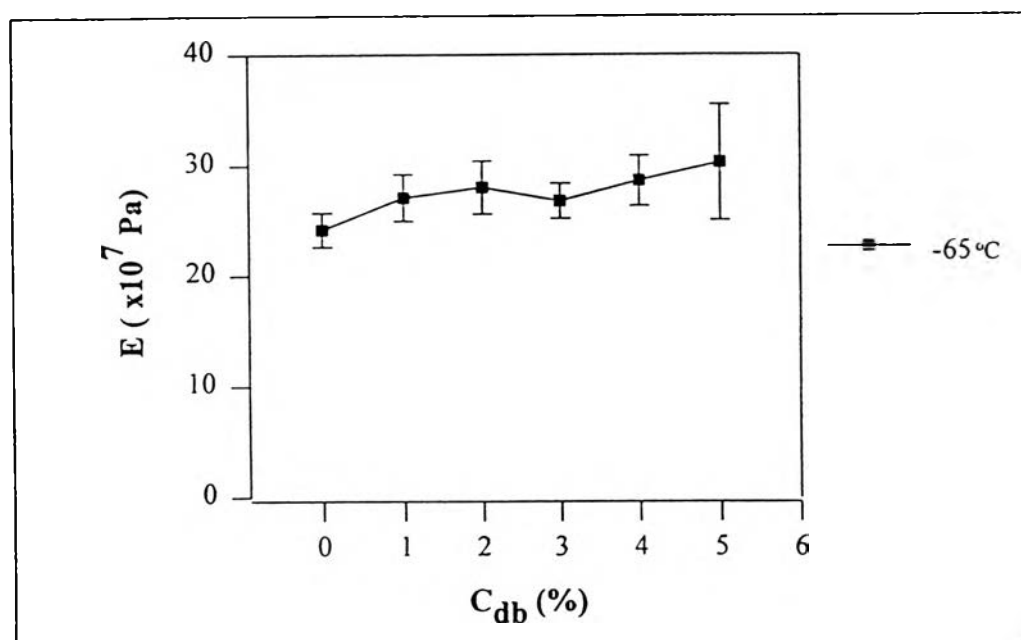


Figure 3.11 Effect of the diblock copolymer content on the Young's modulus of PPO/PI (40/60) blends at -65 °C.

Beyond 3 % of the diblock copolymer. The Young's modulus does not remain the same as in the of PS/P(S-b-I)/PI blends. The effect of exothermic interaction between the PS segment and PPO homopolymer that does not exist in the case of PS homopolymer can show a large influence, transferring of hard property of PPO to the blends and inducing the Young's modulus to increase even though all polymers are in the glassy state.

3.3 Strain Rate

The strain rate is the rate of deformation. We studied two regimes : linear elastic regime and nonlinear elastic regime (for PS/PI blends only). The strain rate was examined by using the highest force rate of 500 mN/min to minimize relaxation of the samples. The composition of PS/PI or PPO/PI blends was fixed at 40/60 and the diblock copolymer concentration was varied from 0 wt % to 5 wt %.

3.3.1 Effect of the diblock copolymer content on the strain rate of PS/PI (40/60) blends

a) Linear elastic regime

The strain rate, in linear elastic regime, was determined from a fixed stress rate divided by the Young's modulus.

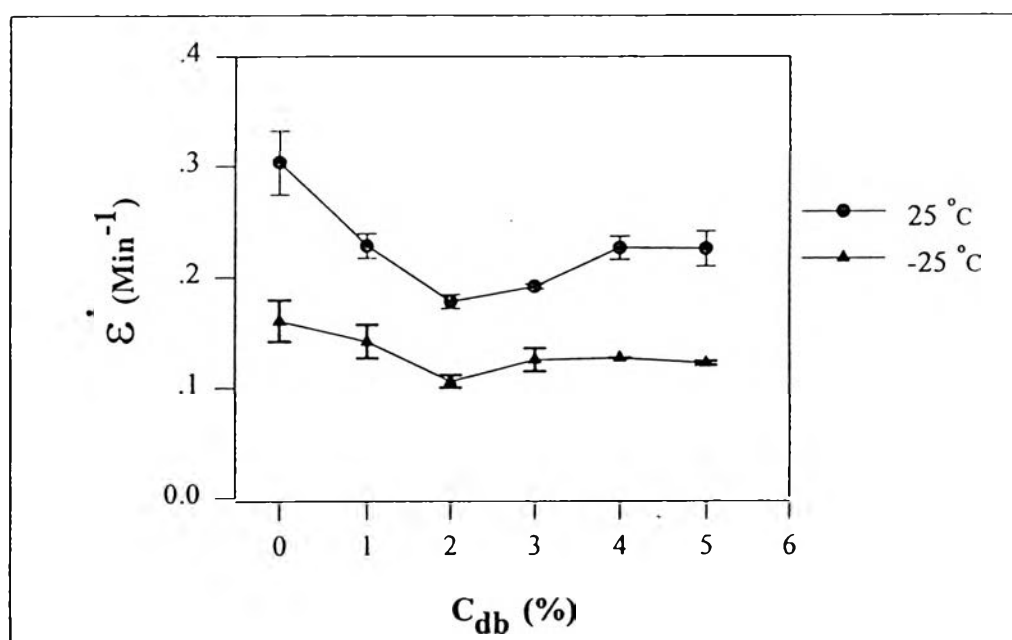


Figure 3.12 Effect of the diblock copolymer content on the strain rate of PS/PI (40/60) blends at 25 °C and -25 °C.

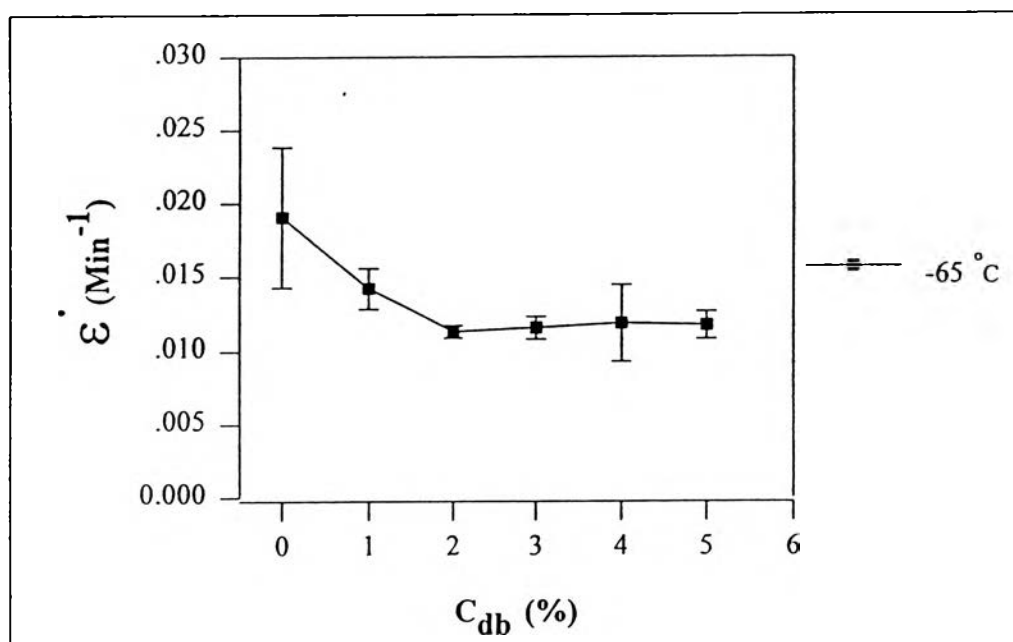


Figure 3.13 Effect of the diblock copolymer content on the strain rate of PS/PI (40/60) blends at -65 °C.

Figure 3.12 shows the effect of the diblock copolymer content on the strain rate of the blends at 25 °C and -25 °C. At these temperatures, PS is in the glassy state and PI is in the rubbery state. It can be seen that the strain rate decreases with the diblock copolymer, reaching a minimum value at 2 wt % diblock copolymer. Next the strain rate increases as more diblock copolymer is added. Between 4 wt % to 5 wt % of the diblock copolymer, the strain rate seems to be nearly constant.

Figure 3.13 shows the effect of the diblock copolymer content on the strain rate of the blends at -65 °C. At this temperature, both of PS and PI phases are in the glassy state. From figure 3.13 shows that the strain rate decreases with addition of the diblock copolymer up to 2 wt % . Beyond 2 wt % of the diblock copolymer, the strain rate does not change very much.

The ideal interfacial morphology models of Figures 3.12 and 3.13 are identical to that of Figure 3.7. The interpretations for the strain rate of Figures

3.12 and 3.13 are similar to the Young's modulus results as shown in the Figures 3.6 and 3.8 respectively.

b) Nonlinear elastic regime

The strain rate, in the nonlinear elastic regime was calculated from the model as follows :

$$\dot{\varepsilon} = \dot{\varepsilon}_v + \dot{\varepsilon}_E + \dot{\varepsilon}_{IN}, \quad (3.1)$$

where $\dot{\varepsilon}$ is total strain rate, $\dot{\varepsilon}_v$ is strain rate of viscous part, $\dot{\varepsilon}_E$ is strain rate of elastic part, and $\dot{\varepsilon}_{IN}$ is strain rate induced by interfacial interaction at the

interface (interaction term). The strain rate $\dot{\varepsilon}$ was obtained numerically from

the strain vs. time curves as follows :

$$\dot{\varepsilon} \cong (\varepsilon_{i+1} - \varepsilon_{i-1})/2\Delta t, \quad (3.2)$$

$$\Delta t \text{ was calculated from } \Delta t = t_{i+1} - t_i, \quad (3.3)$$

$$\text{and } t = 1/\omega, \quad (3.4)$$

$$\text{then } \dot{\varepsilon}_v \text{ was calculated from } \dot{\varepsilon}_v = \sigma/\eta', \quad (3.5)$$

$$\text{and } \eta' \text{ was obtained from } \eta' = E''/\omega, \quad (3.6)$$

$$\text{and } \dot{\varepsilon}_E = \dot{\sigma}/E, \quad (3.7)$$

where σ is stress, η' is viscosity, E'' is loss modulus, ω is the frequency, $\dot{\sigma}$ is stress rate, E is Young's modulus and t is the transient time.

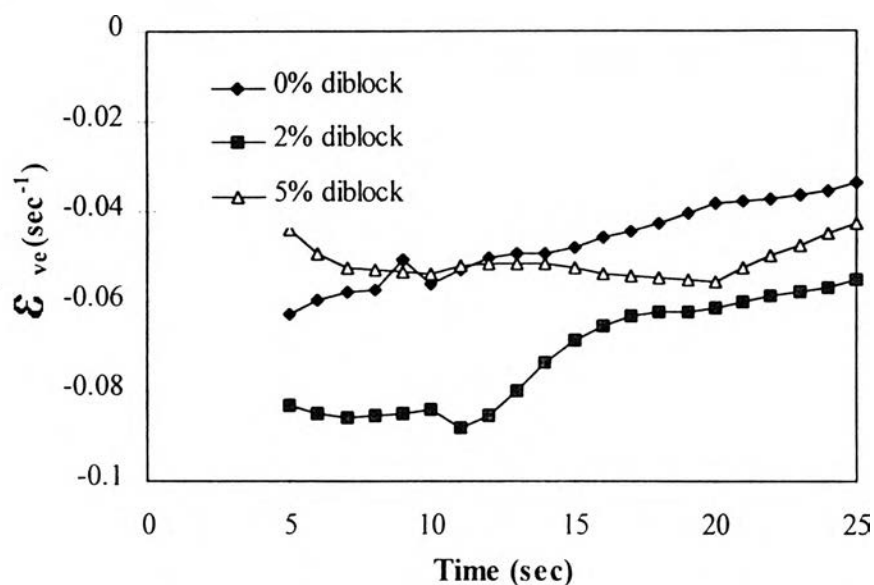


Figure 3.14 The strain rate induced by the interfacial interaction at the interface of the PS/PI (40/60) blends as a function of diblock copolymer and time at 25 °C.

Figure 3.14 shows the strain rate strain rate induced by the interfacial interaction of PS/PI (40/60) blends as a function of diblock copolymer and time at 25 °C. At this temperature, PS phase is in the glassy state and PI is in the rubbery state.

From this plot, the strain rate induced by the interfacial interaction of PS/PI blends with addition of 0 wt %, 2 wt % and 5 wt % of the diblock copolymer increase with time. At 2 wt % and 5 wt % of the diblock copolymer, the strain rate induced by the interfacial interaction are more negative than 0 wt % of the diblock copolymer; implying more resistance to stretching.

3.3.2 Effect of the diblock copolymer content on the strain rate of PPO/PI (40/60) blends

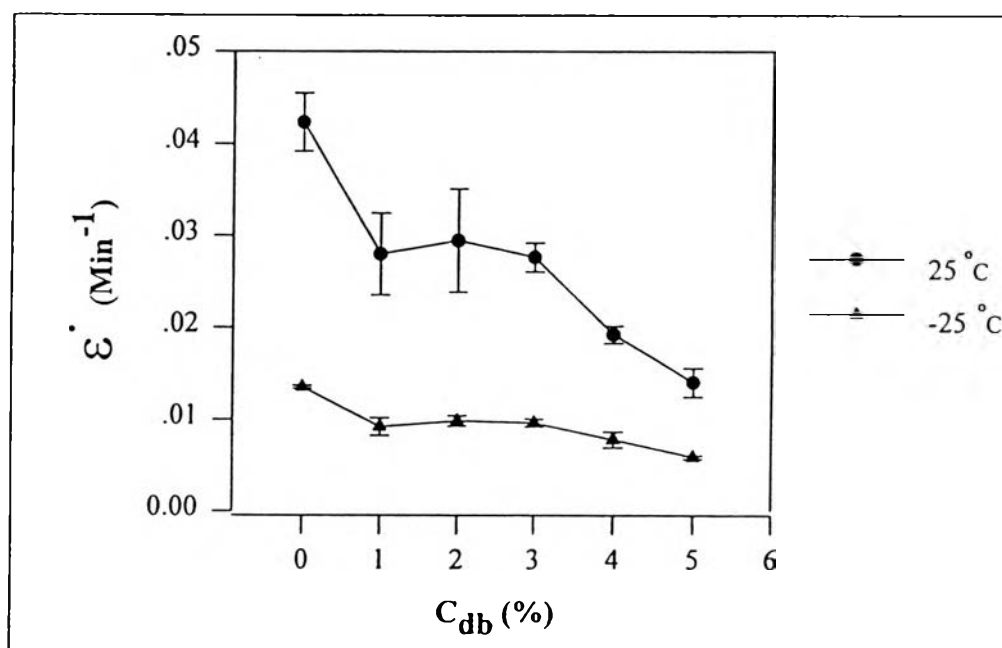


Figure 3.15 Effect of the diblock copolymer content on the strain rate of the PPO/PI (40/60) blends at 25 °C and -25 °C.

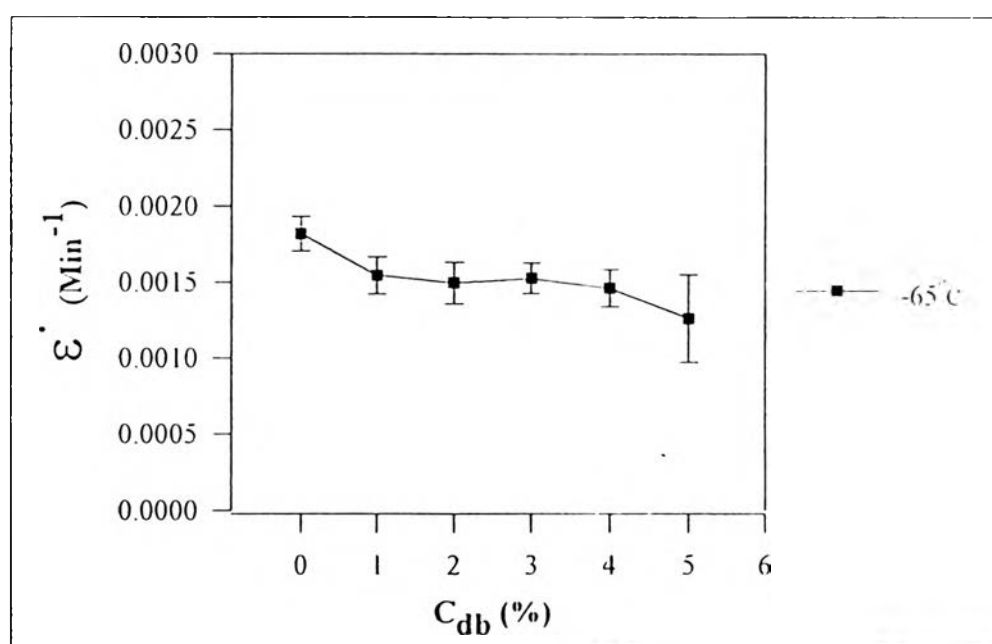


Figure 3.16 Effect of the diblock copolymer content on the strain rate of PPO/PI (40/60) blends at -65 °C.

Figure 3.15 depicts effect of the diblock copolymer content on the strain rate of the blends at 25 °C and -25 °C. At these temperatures, PPO is in the glassy state and PI is in the rubbery state. From Figure 3.15, at 1 % diblock copolymer, strain rate decreases as the diblock copolymer is added. Next, the strain rate seems to be constant from 1 wt % to 3 wt % of the diblock copolymer. Beyond 3 wt % of the diblock copolymer, the strain rate decreases as more diblock copolymers are added.

Figure 3.16 depicts the effect of the diblock copolymer content on the strain rate of the blends at -65 °C. For this condition all polymers are in the glassy state. This figure shows that the strain rate decreases with 1 wt % of the diblock copolymer. Between 1 wt % to 3 wt % of the diblock copolymer, the strain rate remains the same. Beyond 3 wt % of the diblock copolymer, the strain rate decreases as the diblock copolymer is added.

The ideal interfacial morphology models of Figures 3.15 and 3.16 are identical to Figure 3.10. The explanation of the results in Figures 3.15 and 3.16 is similar to that of the Young's modulus results as shown in Figures 3.9 and 3.11 respectively.

Table 3.3 compares the reduction in the strain rate in the linear elastic regime for 1 wt % of the diblock copolymer on the PS/PI and PPO/PI blends at various temperatures. The reduction in the strain rate of the PPO/PI blends with 1 wt % of the diblock copolymer is greater than those of the PS/PI blends, except at -65 °C. This can imply that PS segments can penetrate and entangle with the PPO homopolymers better than that of PS homopolymers leading to a better transfer of stress across the interface. So, the reduction of the strain rate of the PPO/PI blends we can infer the influence of the exothermic heat of reaction.

Table 3.3 Reduction of strain rate in the linear elastic regime for 1 wt % of the diblock copolymer on PS/PI (40/60) and PPO/PI(40/60) at various temperatures

| Temp (°C) | Strain rate of PS/PI (40/60) | | | Strain rate of PPO/PI (40/60) | | |
|-----------|------------------------------|--------|-------------|-------------------------------|--------|-------------|
| | 0% db | 1% db | % reduction | 0% db | 1% db | % reduction |
| -65 | 0.0190 | 0.0142 | 25.26 | 0.0018 | 0.0015 | 15.38 |
| -50 | 0.1044 | 0.0808 | 22.61 | 0.0088 | 0.0064 | 27.29 |
| -35 | 0.1553 | 0.1080 | 30.47 | 0.0129 | 0.0089 | 31.06 |
| -25 | 0.1661 | 0.1420 | 11.56 | 0.0135 | 0.0092 | 31.80 |
| -10 | 0.1969 | 0.1681 | 14.65 | 0.0204 | 0.0159 | 22.32 |
| 0 | 0.2118 | 0.1777 | 16.13 | 0.0215 | 0.0165 | 23.07 |
| 10 | 0.2568 | 0.1884 | 26.60 | 0.0332 | 0.0196 | 41.15 |
| 25 | 0.3034 | 0.2284 | 24.71 | 0.0423 | 0.0280 | 33.88 |

3.4 Yield Stress

Yield stress is the stress at which plastic deformation initiates. Yield stress was obtained from the initial stress strain curved with a line offset of 0.2 % from the origin. The composition of PS/PI or PPO/PI blends was fixed at 40/60 and diblock copolymer concentration was varied from 0-5 wt %. The yield stress was examined by using a force rate at 10 mN/min; that is a small force rate. So during extension, there was enough time for the chain molecules to relax and we obtained an equilibrium stress-strain curve.

3.4.1 Effect of the diblock copolymer content on the yield stress of PS/PI (40/60) blends

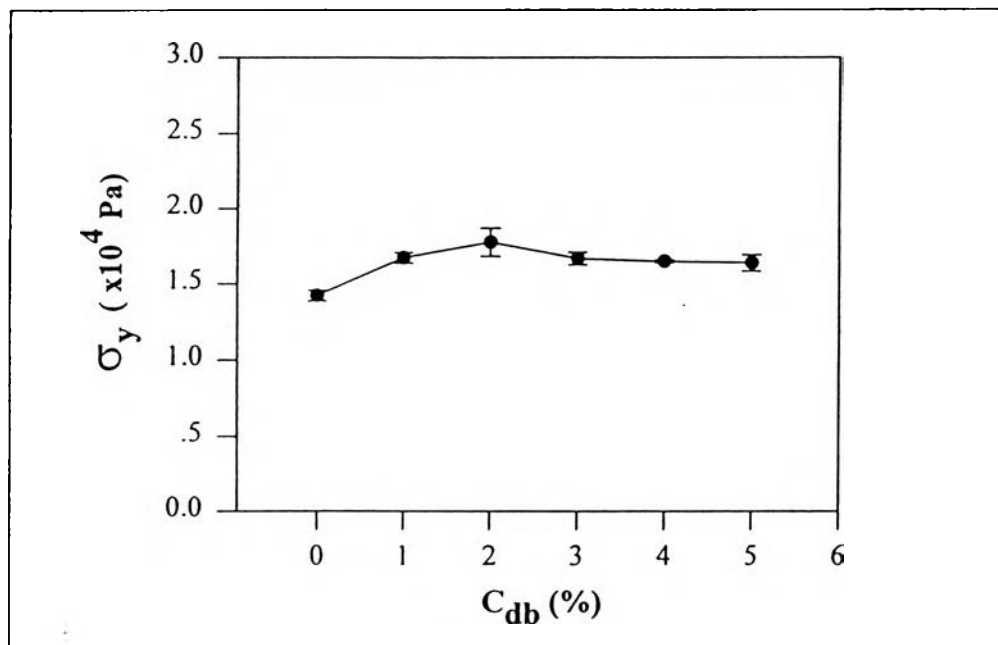


Figure 3.17 Effect of the diblock copolymer content on the yield stress of PS/PI (40/60) blends at 25 °C.

Figure 3.17 depicts the effect of the diblock copolymer content on the yield stress of the blends. It can be seen that the yield stress increases with an addition of diblock copolymer until reaching a maximum value at 2 wt % of the diblock copolymer. After that the yield stress decreases toward a nearly constant value as more diblock copolymer is added.

Between 0 wt % to 2 wt % of the diblock copolymer, the extent of penetration of the PS segments to PS homopolymer is better than the PI segments to the PI homopolymers. Because the molecular weight ratio of homopolymer to block segment is 0.74 for PS/PS, and 13.7 for PI/PI. This means that on the PS/PS interface, there is a better entanglement which may effect the deformation of the rubber phase. Therefore the yield stress increases.

Beyond 2 wt % of the diblock copolymer, the PS segment penetration has saturated. The entanglement of PI segments and PI homopolymers became equally dominant. The yield stress is more influenced by the rubber phase. But the rubber has a low yield stress, hence the yield stress of the blend is lowered.

Between 3 wt % to 5 wt % of the diblock copolymer. A balance between PS and PI penetrations has been reached. Therefore the yield stress is a balance between the two phases and independent of the diblock copolymer content.

3.4.2 Effect of the diblock copolymer content on the yield stress of PPO/PI (40/60) blends

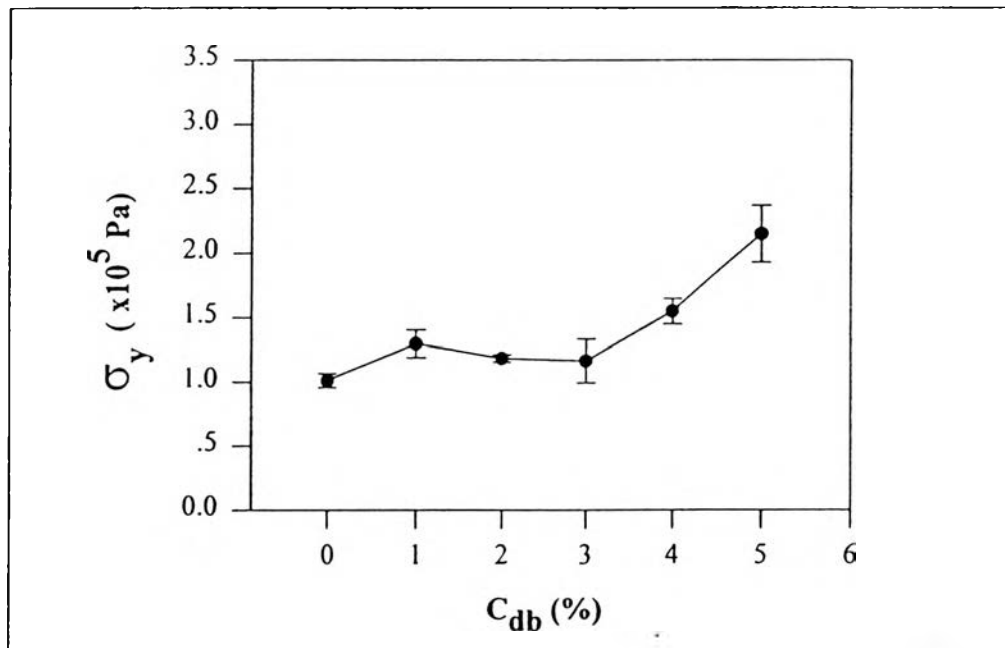


Figure 3.18 Effect of the diblock copolymer content on the yield stress of PPO/PI (40/60) blends at 25 °C.

Figure 3.18 depicts the effect of the diblock copolymer content on the yield stress of the blends. The yield stress increases with 1 wt % of the

diblock copolymer. Between 1 wt % to 3 wt % of the diblock copolymer, the yield stress remains the same. Beyond 3 wt % of the diblock copolymer, the yield stress increases as the diblock copolymer is added.

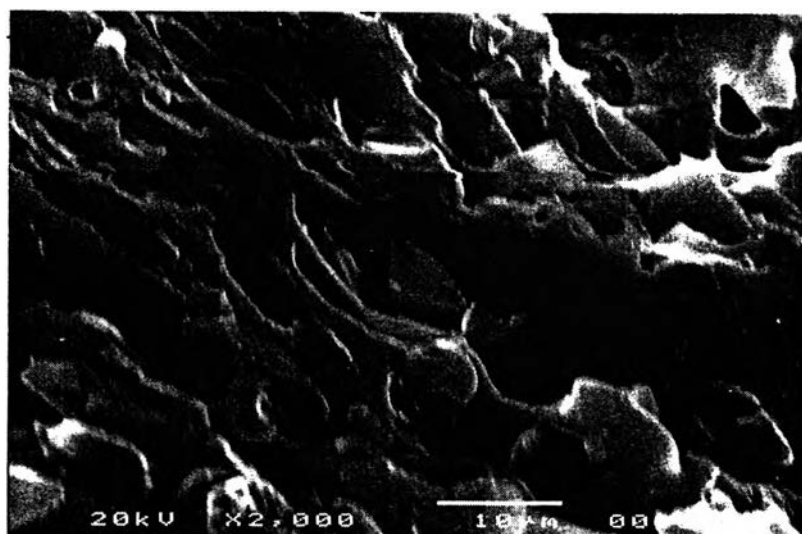
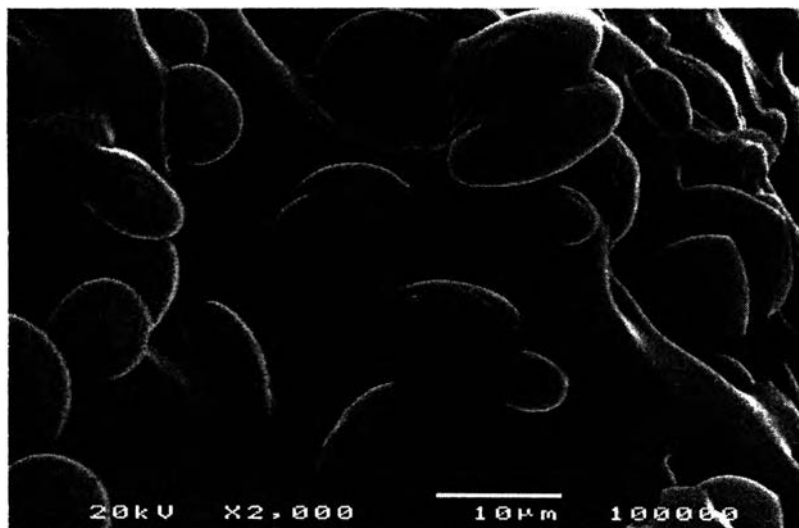
Below 1 wt % of the diblock copolymer, the extent of penetration of the PS segments to the PPO homopolymers is better than that of the PI segments. Because the molecular weight ratio of homopolymer to block copolymer of PPO/PS (0.74) is lower than PI/PI (13.7). The entanglement of PS segments and PPO homopolymers became influential on the yield stress, it induces the increase of the yield stress.

Between 1 wt % to 3 wt % of the diblock copolymer. There is a balance in the penetration of the PS and PI segments into the homopolymers. So the yield stress is a balance between the two phases, and independent of the diblock copolymer content.

Between 3 wt % to 5 wt % of the diblock copolymer, the yield stress increases as diblock copolymer is added. Following the interaction of the PS and PPO is the exothermic heat of mixing which introduces a driving force for the PS segments to become dissolved in the more compatible PPO homopolymers. Since the PPO and PS are rigid, the yield stress is expected to increase as diblock copolymer is added.

3.5 Fracture Surface Morphology

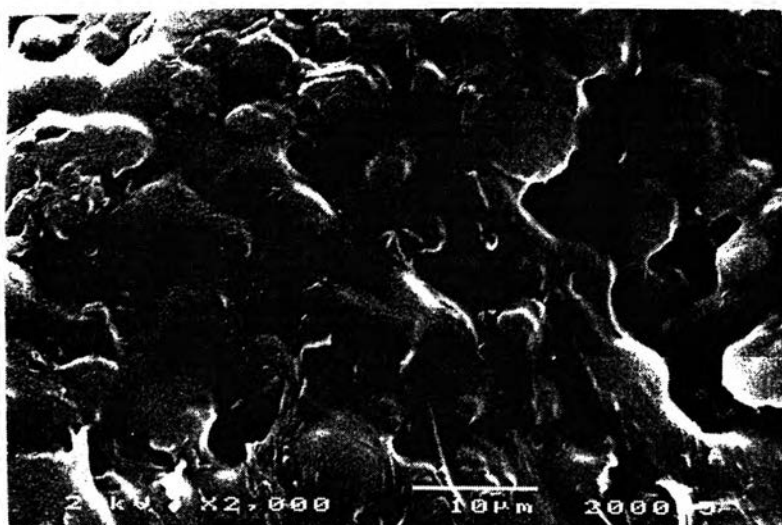
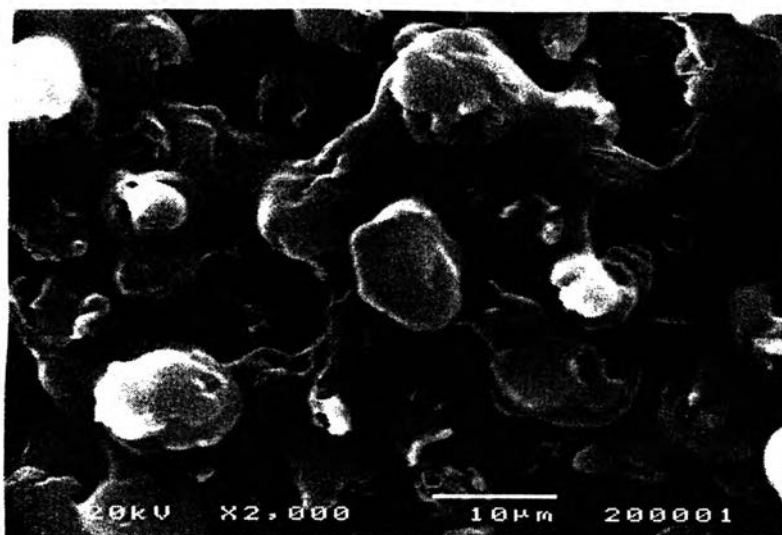
The sample film was fractured in a liquid nitrogen. For coating samples, the samples were mounted on stubs on the sputting device. The samples were coated with sputtered gold for 3 min. Coated sample morphology was observed by SEM an accelerating voltage of 20 kV and a magnification of 2000.



The SEM photographs in Figure 3.19 are the fracture surfaces of two PS/PI (40/60) blends, uncompatibilized and compatibilized with 5 wt % of the diblock copolymer. Without the diblock copolymer [Figure 3.19 (a)], the fracture of the sample apparently produced a clean separation between the PS dispersed phase from the PI matrix. It can be seen that the particle shape of the PS dispersed phase is spherical like. With the diblock copolymer [Figure 3.19 (b)], the diblock copolymer concentrated at the interface between PS and PI phase and adhered to both phases. The particle shape of the PS dispersed domain is altered to be ellipse shape.

The morphology pictures were consistent with Young's modulus and yield stress. Between 0-2 wt % diblock copolymer, we have seen that the Young's modulus increases as diblock copolymer is added. The added diblock copolymer allows a better stress transfer between the two immiscible phases without changing the blend morphology. For 5 wt % diblock copolymer, the shape of PS dispersed domain is altered to an ellipse shape and a change in the blend morphology occurs. Since elongated structure or an ellipse has a larger interfacial tension than a sphere, we can expect that the ability to transfer stress between the two phases is reduced. This is consistent with our data that the Young's modulus attains an asymptotic value with 5 wt % diblock copolymer. There is a balance between the effect of adhesion due to the diblock copolymer with a larger interfacial area and the effect of an increase in the interfacial tension.

It is also possible that the particle size of the PS dispersed domain is reduced with the addition of 5 wt % diblock copolymer. Therefore we expect a lesser interfacial area of PS domains is available to transfer the stress and hence a decline in the Young's modulus toward its asymptotic value.



SEM photographs in Figures 3.20 (a) and (b) are the fracture surfaces of the PPO/PI (40/60) blends uncompatibilized and compatibilized with 5 wt % of the diblock copolymer respectively. We can not discern any difference between the two pictures. The particle shape of the PPO dispersed domain is apparently unaltered with addition of 5 wt % diblock copolymer.

Within this range of diblock content, the compatibilizer enhances the stress transfer between the two immiscible phases without altering the blend morphology. This picture is consistent with our data which demonstrates that the Young's modulus increases monotonically with the diblock copolymer content.